Eur. Phys. J. Special Topics **228**, 1969–1981 (2019)

https://doi.org/10.1140/epjst/e2019-800222-7

THE EUROPEAN PHYSICAL JOURNAL SPECIAL TOPICS

Regular Article

Antimonotonicity and multistability in a fractional order memristive chaotic oscillator

Chao-Yang Chen[1,2], Karthikeyan Rajagopal[3], Ibrahim Ismael Hamarash[4], Fahimeh Nazarimehr[5,a], Fawaz E. Alsaadi[6], and Tasawar Hayat[7,8]

[1] School of Information and Electrical Engineering, Hunan University of Science and Technology, Xiangtan 411201, P.R. China
[2] Center for Polymer Studies and Department of Physics, Boston University, Boston, MA 02215, USA
[3] Center for Nonlinear Dynamics, Defence University, Bishoftu, Ethiopia
[4] Department of Computer Science and Engineering, University of Kurdistan-Hewler, Erbil, Iraq
[5] Department of Biomedical Engineering, Amirkabir University of Technology, 424 Hafez Ave., Tehran 15875-4413, Iran
[6] Department of information Technology, Faculty of Computing and IT, King Abdulaziz University, Jeddah, Saudi Arabia
[7] Department of Mathematics, Quaid-I-Azam University 45320, Islamabad 44000, Pakistan
[8] NAAM Research Group, King Abdulaziz University, Jeddah, Saudi Arabia

Received 9 December 2018 / Received in Final form 5 February 2019
Published online 14 October 2019

Abstract. A memristor diode bridge chaotic circuit is proposed in this paper. The proposed oscillator has only one nonlinear element in the form of memristor. Dynamical properties of the proposed oscillator are investigated. The fractional order model of the oscillator is designed using Grünwald–Letnikov (GL) method. Bifurcation diagrams are plotted which shows that the proposed oscillator exhibits multistability. Finally, the antimonotonicity property of the fractional order oscillator is discussed in detail with two control parameters. Such property has not been explored for fractional order systems before.

1 Introduction

In the last three decades a lot of attention has been given to dynamical systems with elegant mathematical forms. In 1994, Sprott proposed a list of simplest 3-dimensional chaotic systems [1]. Those systems have been the source of inspiration of many new simple chaotic systems [2–4]. Finding chaotic systems with special properties is very interesting since it can help us to understand the generation of chaotic attractors. There are many studies on designing chaotic flows with special structural properties such as systems with no equilibrium point [5–8], stable equilibria [9–12], line of equilibria [13], curve-equilibrium [14,15], surface-equilibrium [16–18], and infinite equilibrium points [19–21]. Chaotic systems with other properties such as fractional-order equations [22–24], multi-scroll attractors [25,26], megastability [27–30], and extreme multistability [31–34] are also attractive. Multistability in a

[a] e-mail: fahimenazarimehr@yahoo.com

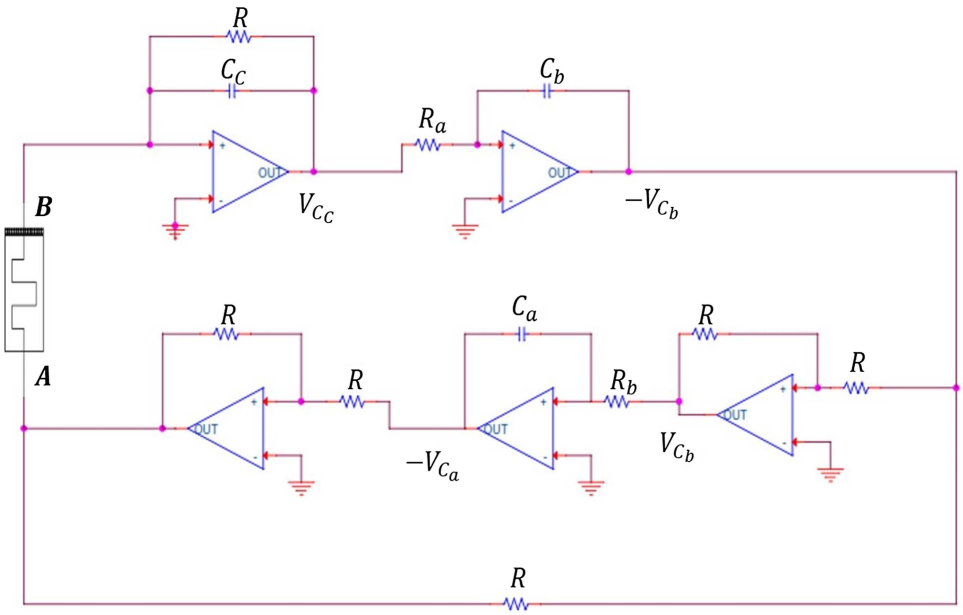

Fig. 1. Circuit structure of MDBO.

new 4-dimentional chaotic system has been investigated in [35]. In [31] multistable memristor based Chua's hyperchaotic system with plane of equilibria has been studied.

There are many categorization of dynamical systems based on different properties. One of them categorizes dynamical systems into two groups, systems with self-excited or systems with hidden attractors [36,37]. This categorization is based on the basin of attractions of attractors. A self-excited attractor can be found using initial conditions around an unstable equilibrium while hidden attractors cannot [38,39]. A time varying controller for the synchronization of hidden chaotic attractors has been proposed in [40].

Memristive chaotic and hyperchaotic systems have attracted lot of attentions [41,42]. Many studies in the context of nonlinear dynamic have been done in this area [43–48]. Chaotic dynamic of a memristive Wien-bridge oscillator has been studied in [49]. Also, fractional order chaotic systems have been a hot topic [50]. Although there are some chaotic circuits recently published, only a few focused on dynamical behaviors of the systems with fractional orders [51–53]. Motivated by this, we investigate a chaotic circuit with a first order memristor. In Section 2, the fractional order model of memristive diode bridge oscillator is introduced. In Section 3, we discuss the dynamics and multistability properties of the model. Conclusions and discussion are given in the last section.

2 Fractional order memristive diode bridge oscillator (FOMDBO)

Memristive based chaotic oscillators have been discussed widely in literature. We have derived the proposed memristive diode bridge oscillator (MDBO) circuit by modifying the jerk system proposed in [54]. We have replaced the two diode element with a memristor whose equivalent circuit is derived using a four diode bridge. The electronic circuit of the proposed system is presented in Figure 1. The circuit has only one nonlinear element. That element is in the form of the memristor if we assume

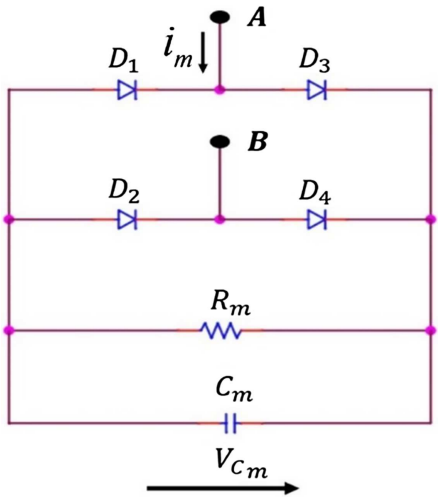

Fig. 2. Diode bridge equivalent circuit of the memristor with a first order RC filter.

that all the operational amplifiers operate in the linear region (ideal) and has three integrators and two inverting amplifiers.

To derive a new mathematical model of the circuit shown in Figure 1, we use the generalized memristor which consist of a first order filter with a diode bridge [55] as shown in Figure 2. All four diodes are chosen to be identical and the values of R_m and C_m are chosen such that the system shows chaotic oscillations.

The mathematical model of the current and voltage are given by,

$$\begin{aligned} i_m &= 2I_s e^{-\alpha V_{C_m}} \sinh(\alpha V_{C_m}) \\ \frac{dV_{C_m}}{dt} &= \frac{2I_s R(e^{-\alpha V_{C_m}} \cosh(\alpha V_{C_m}) - 1) - V_{C_m}}{RC_m} \end{aligned} \tag{1}$$

where $\alpha = \frac{1}{2\pi\eta V_T}$ and η, V_T are the emission coefficient and thermal voltage respectively [56]. To derive the state equations of the circuit, let us define the voltages across the capacitors C_a, C_b, C_c, C_m as $V_{C_a}, V_{C_b}, V_{C_c}, V_{C_m}$ respectively. Applying Kirchoffs voltage and current laws to the circuit, the four state equations can be derived as,

$$\begin{aligned} C_a \frac{dV_{C_a}}{dt} &= \frac{V_{C_b}}{R_b} \\ C_b \frac{dV_{C_b}}{dt} &= \frac{V_{C_c}}{R_b} \\ C_c \frac{dV_{C_c}}{dt} &= \frac{V_{C_a}}{R} - \frac{V_{C_b}}{R_a} - \frac{V_{C_c}}{R} - 2I_s e^{-\alpha V_{C_m}} \sinh(\alpha V_{C_m}) \\ C_m \frac{dV_{C_m}}{dt} &= \frac{2I_s R(e^{-\alpha V_{C_m}} \cosh(\alpha V_{C_m}) - 1) - V_{C_m}}{R}. \end{aligned} \tag{2}$$

To derive the dimensionless state equations of (2), we assign the state variables as $x = V_{C_a}$, $y = V_{C_b}$, $z = V_{C_c}$, $w = V_{C_m}$. The parameters are taken as $a_1 = \frac{1}{RC_a}$, $a_2 = \frac{1}{RC_b}, a_3 = \frac{1}{RC_c}, a_4 = -\frac{1}{RC_c}$, $a_5 = -\frac{1}{R_a C_c}$, $a_6 = -\frac{2I_s}{C_m}$, $a_7 = \alpha$, $a_8 = \frac{1}{C_m}$,

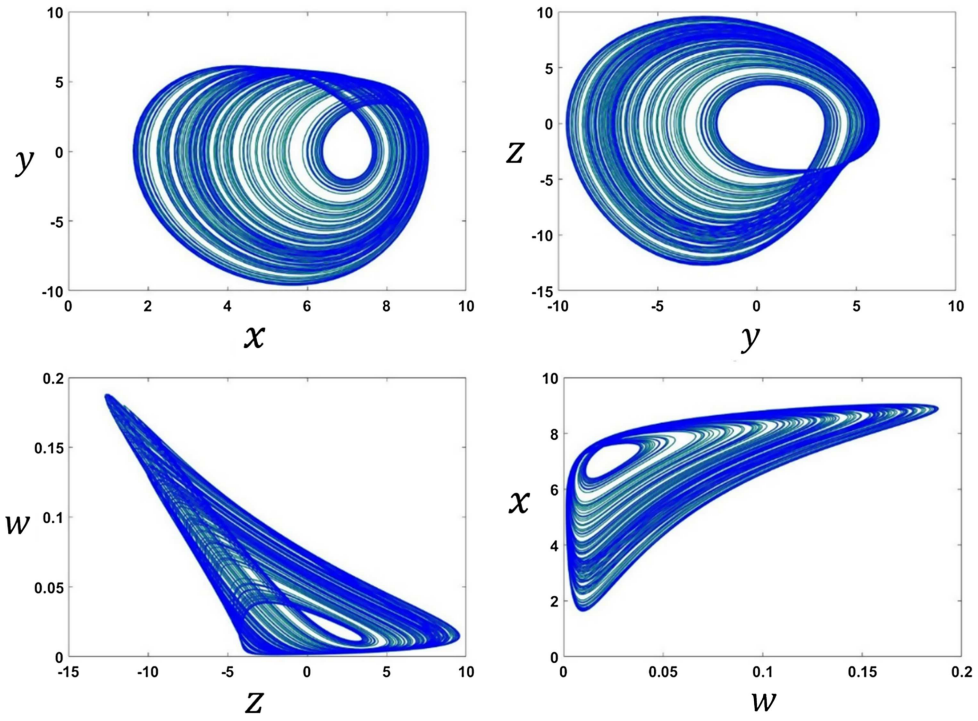

Fig. 3. Four projections of the strange attractor of the MDBO system.

$a_9 = -\frac{1}{R_m C_m}$. Applying these assumptions, the dimensionless state equation of the MDBO system can be derived as,

$$\begin{aligned} \dot{x} &= a_1 y \\ \dot{y} &= a_2 z \\ \dot{z} &= a_3 x + a_4 z = a_5 y + a_6 e^{-a_7 w} \sinh\left(\frac{a_7 x}{3}\right) \\ \dot{w} &= a_8 \left((-a_6)\left(e^{-a_7 w} \cosh\left(\frac{a_7 x}{3}\right) - 1\right)\right) + a_9 w. \end{aligned} \tag{3}$$

The MDBO system shows strange attractor in parameter values $a_1 = 1$, $a_2 = 2, a_3 = 1, a_4 = -1$, $a_5 = -2.95$, $a_6 = -5.36e{-}5$, $a_7 = 5$, $a_8 = 0.02$, $a_9 = -3$ and initial conditions $[0.1, 0.1, 0.1, 0.1]$. Figure 3 presents the strange attractor of the MDBO system.

The equilibria of the MDBO system can be calculated as follows:

$$\begin{aligned} w &= -\frac{1}{a_7} \ln\left(\frac{-a_3 x}{a_6 \sinh\left(\frac{a_7 x}{3}\right)}\right) \\ 0 &= a_8 \left((-a_6)\left(e^{-a_7 w} \cosh\left(\frac{a_7 x}{3}\right) - 1\right)\right) + a_9 w. \end{aligned} \tag{4}$$

Equation (4) is a transcendental equation and cannot be solved analytically and hence we choose numerical solutions using MATLAB to find the equilibrium points. It can be seen that the MDBO system has a trivial fixed point E_1 at $[0, 0, 0, 0]$ and have two nontrivial equilibrium points E_2, E_3 at $\mp 7.69, 0, 0, 0.0512$. The eigenvalues of the MDBO system at the trivial equilibrium point E_1 are $\lambda_1 = 0.3166, \lambda_{2,3} =$

$-0.6583 \pm 2.4256i, \lambda_4 = -3$ and at nontrivial points E_2, E_3 are $\lambda_{1,2} = 0.5903 \pm 2.9709i, \lambda_3 = -4.1245, \lambda_4 = -1.8203$. As can be observed from the eigenvalues the equilibrium point E_1 is a saddle focus of index-1 and equilibrium points E_2, E_3 are saddle focus of index-2.

In this paper, the fractional order memristive diode bridge oscillator (FOMDBO) has been proposed. The fractional order mathematical model of the proposed system is derived using Grünwald-Letnikov (GL). Let us define the FOMDBO oscillator as,

$$\begin{aligned} D^q x &= a_1 y \\ D^q y &= a_2 z \\ D^q z &= a_3 x + a_4 z + a_5 y + a_6 e^{-a_7 w} \sinh\left(\frac{a_7 x}{3}\right) \\ D^q w &= a_8 \left((-a_6)\left(e^{-a_7 w}\cosh\left(\frac{a_7 x}{3}\right) - 1\right)\right) + a_9 w. \end{aligned} \tag{5}$$

The discrete form of the FOMDBO system is given by,

$$\begin{aligned} x(t_k) &= \left(a_1 y\left(t_{k-1}\right)\right) h^q - \sum_{j=0}^{N} \beta_j^q x(t_{k-j}) \\ y(t_k) &= \left(a_2 z\left(t_{k-1}\right)\right) h^q - \sum_{j=0}^{N} \beta_j^q y(t_{k-j}) \\ z(t_k) &= \left(a_3 x(t_{k-1}) + a_4 z(t_{k-1}) + a_5 y(t_{k-1})\right. \\ &\quad \left. + a_6 e^{-a_7 w(t_{k-1})} \sinh\left(\frac{a_7 x\left(t_{k-1}\right)}{3}\right)\right) h^q - \sum_{j=0}^{N} \beta_j^q z(t_{k-j}) \\ w(t_k) &= \left(a_8\left((-a_6)\left(e^{-a_7 w(t_{k-1})}\cosh\left(\frac{a_7 x\left(t_{k-1}\right)}{3}\right) - 1\right)\right)\right. \\ &\quad \left. + a_9 w\left(t_{k-1}\right)\right) h^q - \sum_{j=0}^{N} \beta_j^q w(t_{k-j}) \end{aligned} \tag{6}$$

where h is the step size, q is the fractional order of the differential equation, and β_j is binomial coefficients required for the numerical simulation. The value of N is taken as the truncation window size L and as k when all the available memory elements are used.

The parameter values are considered as $a_1 = 1$, $a_2 = 2$, $a_3 = -1$, $a_4 = -1$, $a_6 = -5.36e{-}5$, $a_7 = 5$, $a_8 = 0.02$, $a_9 = -3$ and initial conditions are $[0.1, 0.1, 0.1, 0.1]$. Figures 4 and 5 show the chaotic attractor of the FOMDBO system in $a_5 = -2.95$ and $a_5 = -1.9$. For both cases the commensurate fractional orders are kept as $q = 0.99$.

3 Dynamical properties of FOMDBO

3.1 Route to chaos

To discuss the dynamical properties of FOMDBO, bifurcations with respect to changing parameters and fractional order of the system is investigated. The bifurcation parameter has been chosen as a_2 while the other parameters are kept constant as

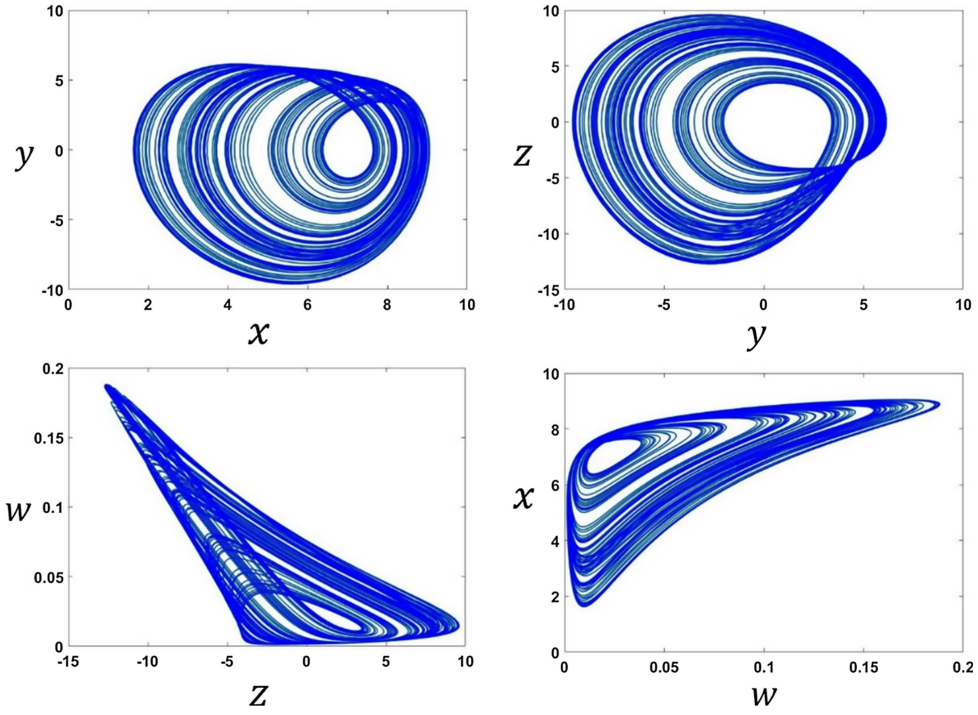

Fig. 4. 2D phase portraits of the FOMDBO in $a_5 = -2.95$.

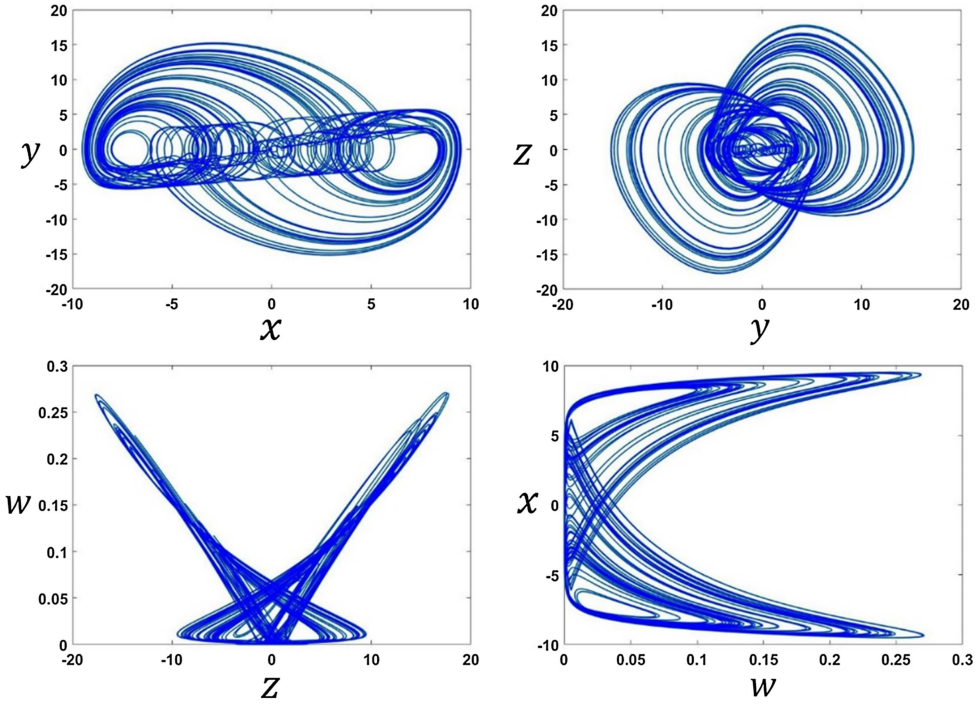

Fig. 5. 2D phase portraits of the FOMDBO system in $a_5 = -1.9$.

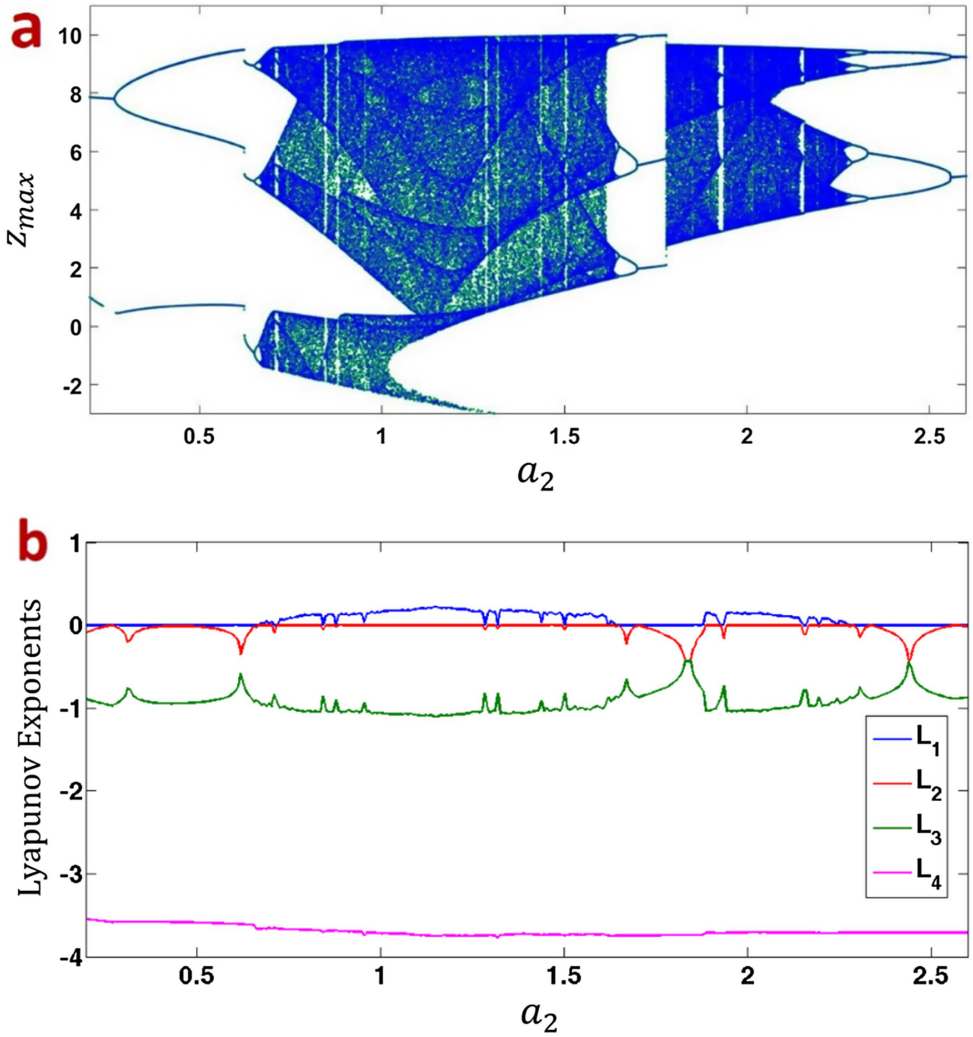

Fig. 6. (a) Bifurcation of the FOMDBO system with respect to changing parameter a_2; and (b) the corresponding Lyapunov exponents.

$a_1 = 1$, $a_3 = -1$, $a_4 = -1$, $a_5 = -2.95$, $a_6 = -5.36e{-}5$, $a_7 = 5$, $a_8 = 0.02$, $a_9 = -3$ and the commensurate fractional order of the system is taken $q = 0.995$. Initial conditions are considered $[0.1, 0.1, 0.1, 0.1]$. Bifurcation diagram of FOMDBO and Lyapunov exponents (LEs) with respect to changing parameter a_2 are shown in Figure 6. The FOMDBO shows a period doubling route to chaos and has creation and annihilation of period doublings which is known as antimonotonicity. This property of the system will be investigated in detail at a later part of this paper.

Next, we investigate bifurcation diagram of FOMDBO with respect to changing commensurate fractional order. In this case, we fix all the other system parameters except a_5 to their respective values (chaotic solution) and initial conditions taken as $[0.1, 0.1, 0.1, 0.1]$. The bifurcation is derived for two conditions, $a_5 = -2.95$ and $a_{5,} = -1.9$ and they are shown in Figures 7a and 7b respectively. In $a_5 = -2.95$, the system shows chaotic oscillations in the interval $0.987 \leq q < 1$ which can be seen in Figures 7a and 7b show antimonotonicity by period doubling in $0.975 \leq q < 0.98$ and reverse route of period doubling in $0.992 \leq q < 0.995$.

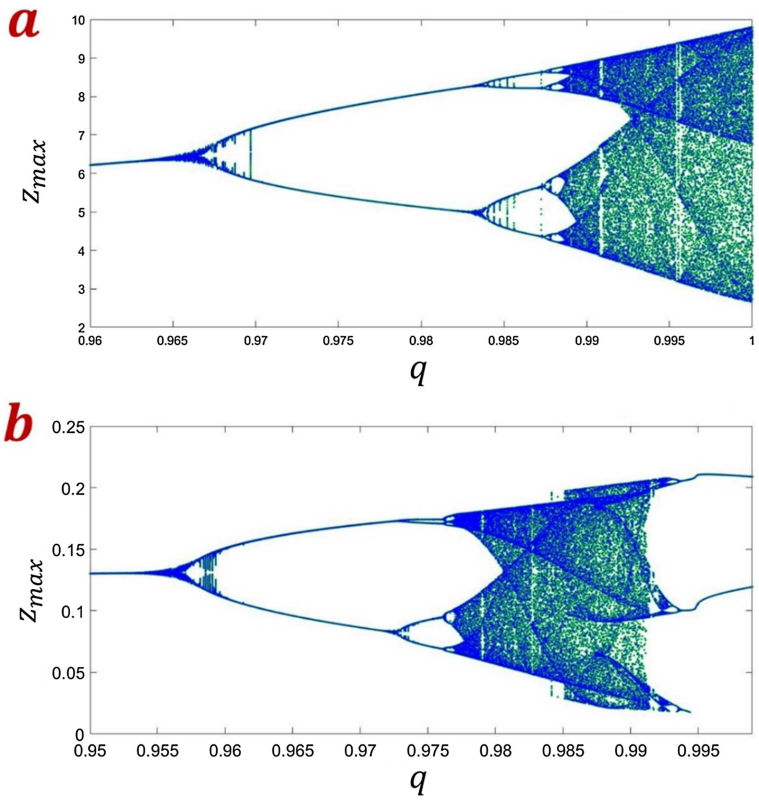

Fig. 7. (a) Bifurcation of the FOMDBO system with respect to changing fractional order q in $a_5 = -2.95$. (b) Bifurcation of the FOMDBO system with respect to changing fractional order q in $a_5 = -1.9$.

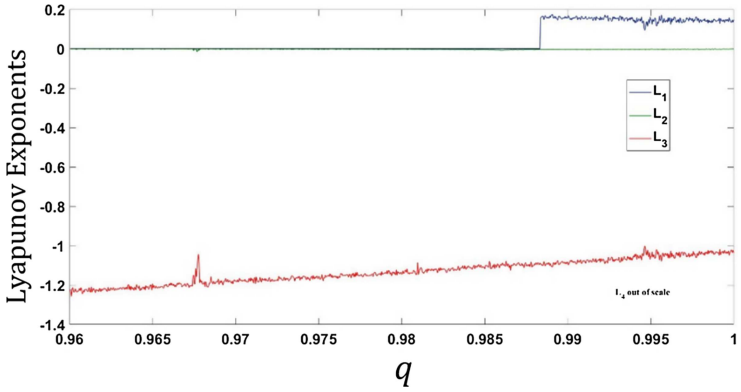

Fig. 8. Lyapunov spectrum of the FOMDBO system in $a_5 = -2.95$ with respect to changing fractional order q.

The Lyapunov exponents (LEs) of the FOMDBO in $a_5 = -2.95$ are shown in Figure 8. Lyapunov exponents are derived using the Wolf's algorithm [57] and the fractional order predictor-corrector [58] solver fde12 [59] instead of the ode solvers [60]. The positive largest Lyapunov exponent proves the existence of chaos in higher values of fractional order q.

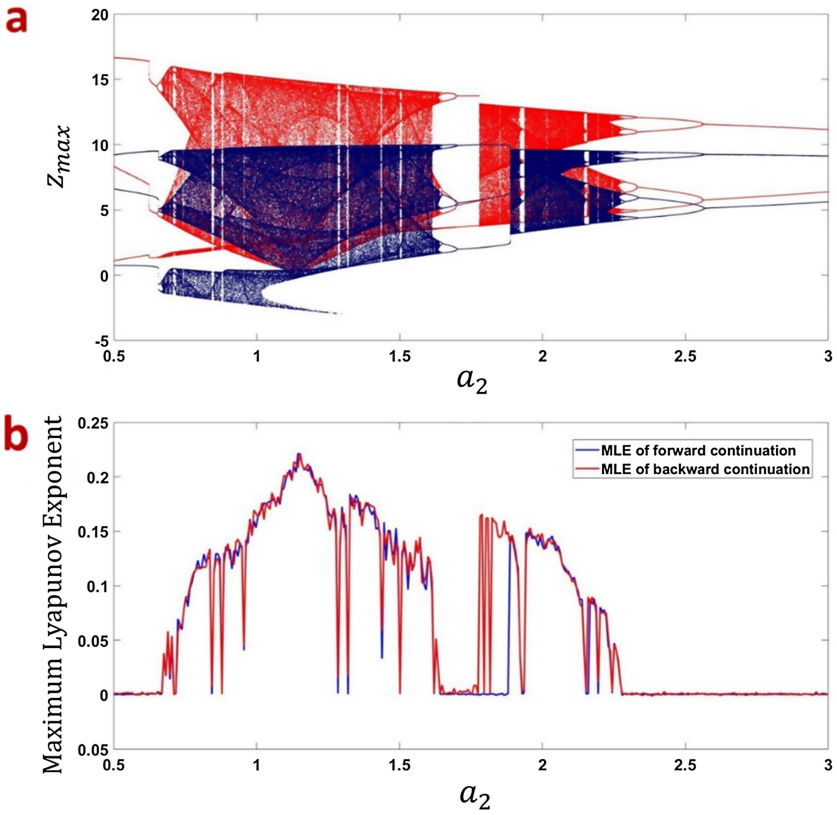

Fig. 9. (a) Bifurcation of the FOMDBO with respect to changing parameter a_2 with forward (blue plot) and backward (red plot) continuation, (b) the corresponding Maximum Lyapunov exponent (MLE) with forward (blue plot) and backward (red plot) continuation.

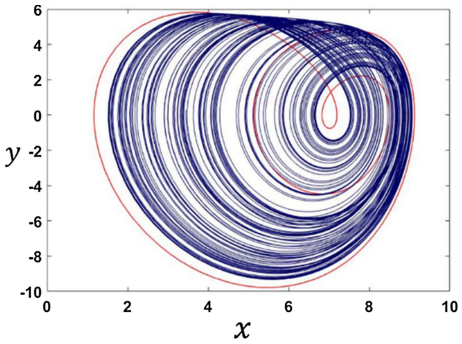

Fig. 10. Coexisting attractors of FOMDBO in $a_2 = 1.82$. Initial conditions are $[7.03, 4.77, 1.05, 0]$ in blue plot and $[6.4, -6.5, -0.59, 0.06]$ in red plot.

3.2 Multistability analysis

In order to investigate multistability of a system, we should track the attractors of the system with different initial conditions. One common way to detect multistability in a dynamical system is plotting bifurcation diagram of the system with forward and backward continuation. Parameter $a_5 = -2.95$, commensurate fractional order taken

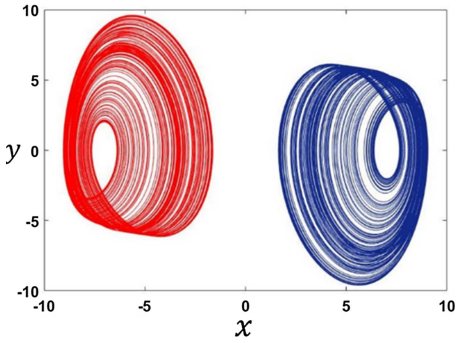

Fig. 11. Coexisting attractors of FOMDBO in $a_2 = 2$. Initial conditions are $[0.1, 0.1, 0.1, 0.1]$ in blue plot and $[-0.1, -0.1, -0.1, -0.1]$ in red plot.

as $q = 0.99$ and the other parameters are fixed to their respective chaotic solutions. In the forward (or backward) continuation method bifurcation diagram is obtained by plotting local maxima of the coordinate z in terms of the parameter that is increased (or decreased) in tiny steps in the range of $0.5 \leq a_2 \leq 3$. The final states at each parameter serves as the initial conditions for the next parameter. Plotting bifurcation diagram with forward and backward continuation represents a simple way to localize the window in which the system develops multistability. In Figure 9, the existence of a chaotic attractor in forward continuation in the interval $1.784 \leq a_2 \leq 1.887$ can be seen while the backward continuation shows period 3 limit cycles in that range. Also, a very narrow band of chaotic attractor can be seen in $2.155 \leq a_2 \leq 2.163$ with forward continuation. But in the backward continuation a period 6 limit cycle can be seen. These claims are well supported by the finite time Lyapunov exponents (only the maximum LE is plotted) shown in Figure 9b. They are calculated using the Wolf's algorithm [57,60–62] with re-initialized initial conditions obtained in forward and backward continuations. So, the proposed FOMDBO system has hysteresis since the bifurcation diagram with forward and backward continuation are different in some interval of parameters. In other words, the system shows bi-stability. Figure 10 shows the coexisting attractor of FOMDBO in $a_2 = 1.82$ and two different initial conditions. The FOMDBO shows a chaotic attractor with coexisting limit cycles as shown with blue and red plots respectively. Figure 11 presents coexisting chaotic attractors in $a_2 = 2$ with two antisymmetric initial conditions.

3.3 Antimonotonicity

The process of period doubling and its inverse route which can occur in the bifurcation diagram of a system is termed as antimonotonicity. To investigate this in detail, we derive the bifurcation of FOMDBO with a_2 and a_5 as the control parameters. The fractional order in this analysis is taken as $q = 0.99$ and we use the forward continuation to plot the bifurcation diagrams. Figures 12a–f show the bifurcation diagrams of the FOMDBO with respect to changing parameter a_2 and in various values of control parameter a_5. The novelty of this study is that such a feature has not been discussed in literatures with fractional order models. The evidence of period doubling route to chaos and its inverse route is clearly seen from the bifurcation plots reported in Figure 12.

4 Conclusions

A fractional order memristor diode bridge oscillator was proposed and dynamical properties of the proposed oscillator have been discussed. The fractional order model

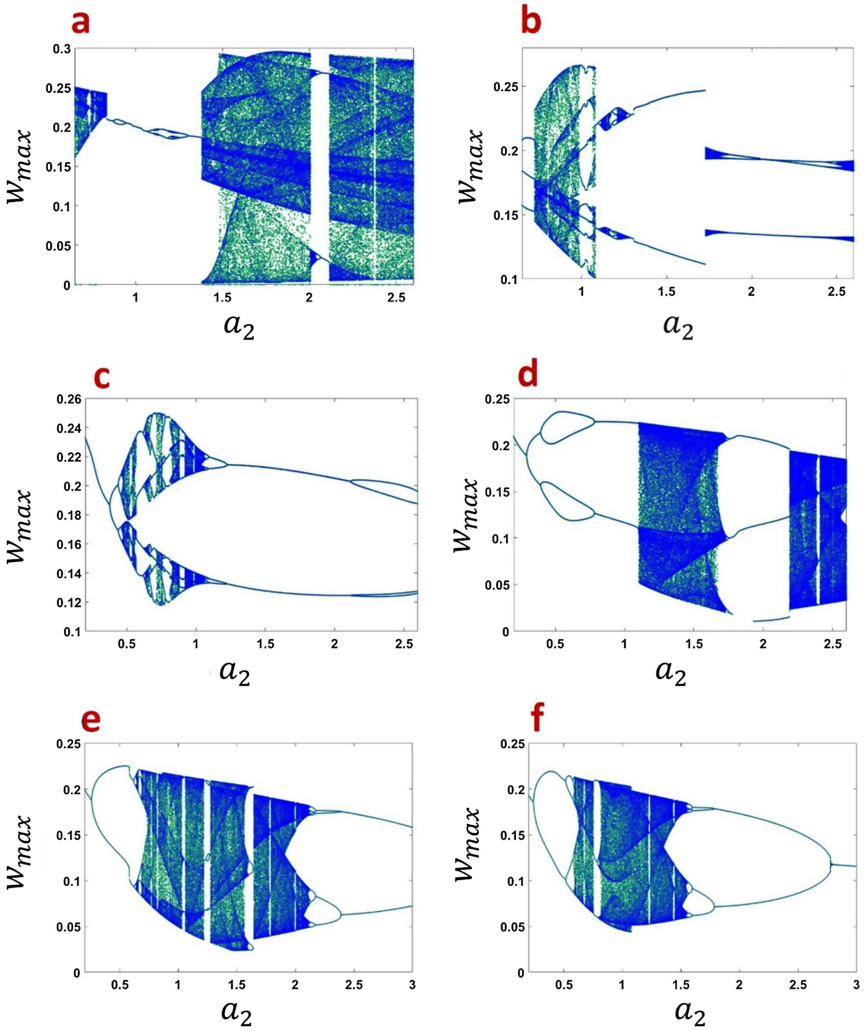

Fig. 12. Bifurcation diagram of FOMDBO with respect to changing a_2 and for different constant values of a_5. (a) $a_5 = -1.7$, (b) $a_5 = -2.2$, (c) $a_5 = -2.5$, (d) $a_5 = -2.8$, (e) $a_5 = -3$, (f) $a_5 = -3.2$.

was derived using Grünwald–Letnikov. FOMDBO system showed multistability and coexisting attractors which were investigated in detail. In addition, the fractional order system exhibited antimonotonicity property which was investigated by keeping two control parameters and deriving the bifurcation plots. As far as we know such properties were not discussed in the literature with fractional order models.

This work was partially supported by the National Natural Science Foundation of China (61503133), the Open Project of MOE Key Laboratory of Image Processing and Intelligence Control (IPIC2015-04), and the Natural Science Foundation of Hunan Province (2016JJ6043). The work was supported by the College of Engineering, Defence University, Ethiopia with partial support from the Center for Nonlinear Dynamics, Defence University, Ethiopia (Grant No.- CND/DEC/2018/1) and partially supported by Iran Science Elites Federation Grant No. M – 97171.

References

1. J.C. Sprott, Phys. Rev. E **50**, R647 (1994)
2. S. Jafari, J.C. Sprott, S.M.R. Hashemi Golpayegani, Phys. Lett. A **377**, 699 (2013)
3. S. Jafari, J.C. Sprott, Chaos Solitons Fractals **57**, 79 (2013)
4. M. Molaie, S. Jafari, J.C. Sprott, S.M.R.H. Golpayegani, Int. J. Bifurc. Chaos **23**, 1350188 (2013)
5. Z. Wei, R. Wang, A. Liu, Math. Comput. Simul. **100**, 13 (2014)
6. V.T. Pham, S. Jafari, C. Volos, X. Wang, S.M.R.H. Golpayegani, Int. J. Bifurc. Chaos **24**, 1450146 (2014)
7. F. Nazarimehr, K. Rajagopal, J. Kengne, S. Jafari, V.T. Pham, Chaos Solitons Fractals **111**, 108 (2018)
8. S. Ren, S. Panahi, K. Rajagopal, A. Akgul, V.T. Pham, S. Jafari, Z. Naturforsch. A **73**, 239 (2018)
9. Z. Wei, I. Moroz, A. Liu, Turk. J. Math. **38**, 672 (2014)
10. V.T. Pham, S. Jafari, T. Kapitaniak, C. Volos, S.T. Kingni, Int. J. Bifurc. Chaos **27**, 1750053 (2017)
11. V.T. Pham, X. Wang, S. Jafari, C. Volos, T. Kapitaniak, Int. J. Bifurc. Chaos **27**, 1750097 (2017)
12. X. Wang, V.T. Pham, S. Jafari, C. Volos, J.M. Munoz-Pacheco, E. Tlelo-Cuautle, IEEE Access **5**, 8851 (2017)
13. J.P. Singh, B. Roy, Nonlinear Dyn. **89**, 1 (2017)
14. V.T. Pham, C. Volos, T. Kapitaniak, S. Jafari, X. Wang, Int. J. Electron. **105**, 385 (2018)
15. S. Panahi, Z. Aram, S. Jafari, V.T. Pham, C. Volos, K. Rajagopal, Pramana **90**, 31 (2018)
16. J.P. Singh, B.K. Roy, S. Jafari, Chaos Solitons Fractals **106**, 243 (2018)
17. S. Jafari, J.C. Sprott, V.T. Pham, C. Volos, C. Li, Nonlinear Dyn. **86**, 1349 (2016)
18. S. Jafari, J.C. Sprott, M. Molaie, Int. J. Bifurc. Chaos **26**, 1650098 (2016)
19. K. Rajagopal, S. Jafari, A. Karthikeyan, A. Srinivasan, B. Ayele, Circuits Syst. Signal Process. **37**, 1 (2018)
20. K. Rajagopal, S. Çiçek, A.J.M. Khalaf, V.T. Pham, S. Jafari, A. Karthikeyan, P. Duraisamy, Z. Naturforsch. A **73**, 609 (2018)
21. E. Tlelo-Cuautle, L.G. De La Fraga, V.T. Pham, C. Volos, S. Jafari, A. de Jesus Quintas-Valles, Nonlinear Dyn. **89**, 1 (2017)
22. C. Li, K. Su, L. Wu, J. Comput. Nonlinear Dyn. **8**, 031005 (2013)
23. C. Li, Y. Tong, Pramana **80**, 583 (2013)
24. Y. Zhang, Phys. Lett. A **377**, 1269 (2013)
25. J. Ma, P. Zhou, B. Ahmad, G. Ren, C. Wang, PLoS One **13**, e0191120 (2018)
26. W. Ai, K. Sun, Y. Fu, Int. J. Mod. Phys. C **29**, 1850049 (2018)
27. J.C. Sprott, S. Jafari, A.J.M. Khalaf, T. Kapitaniak, Eur. Phys. J. Special Topics **226**, 1979 (2017)
28. Y.-X. Tang, A.J.M. Khalaf, K. Rajagopal, V.-T. Pham, S. Jafari, Y. Tian, Chin. Phys. B **27**, 40502 (2018)
29. C. Li, J.C. Sprott, Y. Mei, Nonlinear Dyn. **89**, 2629 (2017)
30. Z. Wei, V.T. Pham, A.J.M. Khalaf, J. Kengne, S. Jafari, Int. J. Bifurc. Chaos **28**, 1850085 (2018)
31. B. Bao, T. Jiang, G. Wang, P. Jin, H. Bao, M. Chen, Nonlinear Dyn. **89**, 1157 (2017)
32. B. Bao, T. Jiang, Q. Xu, M. Chen, H. Wu, Y. Hu, Nonlinear Dyn. **86**, 1711 (2016)
33. B.C. Bao, H. Bao, N. Wang, M. Chen, Q. Xu, Chaos Solitons Fractals **94**, 102 (2017)
34. H. Bao, N. Wang, B. Bao, M. Chen, P. Jin, G. Wang, Commun. Nonlinear Sci. Numer. Simul. **57**, 264 (2018)
35. J.P. Singh, B. Roy, Optik **145**, 209 (2017)
36. N.V. Stankevich, N.V. Kuznetsov, G.A. Leonov, L.O. Chua, Int. J. Bifurc. Chaos **27**, 1730038 (2017)
37. N.V. Kuznetsov, G.A. Leonov, M.V. Yuldashev, R.V. Yuldashev, Commun. Nonlinear Sci. Numer. Simul. **51**, 39 (2017)

38. P.R. Sharma, M.D. Shrimali, A. Prasad, N.V. Kuznetsov, G.A. Leonov, Eur. Phys. J. Special Topics **224**, 1485 (2015)
39. M.-F. Danca, N. Kuznetsov, Chaos Solitons Fractals **103**, 144 (2017)
40. J.P. Singh, B.K. Roy, Trans. Inst. Meas. Control **40**, 3573 (2017)
41. B. Bao, A. Hu, H. Bao, Q. Xu, M. Chen, H. Wu, Complexity **2018**, 3872573 (2018)
42. Y. Zhang, L.F. Lu, Nonlinear Dyn. **77**, 1121 (2014)
43. B. Bao, L. Xu, Z. Wu, M. Chen, H. Wu, Int. J. Electron., **105**, 1159 (2018)
44. Y. Zhang, Nonlinear Dyn. **73**, 2221 (2013)
45. B.C. Bao, P.Y. Wu, H. Bao, H.G. Wu, X. Zhang, M. Chen, Chaos Solitons Fractals **109**, 146 (2018)
46. B.C. Bao, P.Y. Wu, H. Bao, Q. Xu, M. Chen, Chaos Solitons Fractals **106**, 161 (2018)
47. H. Bao, N. Wang, H. Wu, Z. Song, B. Bao, IETE Tech. Rev. **36**, 1 (2019)
48. Q. Xu, Q.L. Zhang, H. Qian, H.G. Wu, B.C. Bao, Int. J. Circuit Theory Appl. **46**, 1917 (2018)
49. H. Wu, B. Bao, Z. Liu, Q. Xu, P. Jiang, Nonlinear Dyn. **83**, 893 (2016)
50. Y. Zhang, G. Luo, Q. Cao, M. Lin, Int. J. Nonlinear Mech. **58**, 151 (2014)
51. X. Wang, S.T. Kingni, C. Volos, V.T. Pham, D. Vo Hoang, S. Jafari, Int. J. Electron. **106**, 109 (2019)
52. K. Rajagopal, F. Nazarimehr, A. Karthikeyan, A. Srinivasan, S. Jafari, Asian J. Control **20** 1979 (2018)
53. K. Rajagopal, A. Akgul, S. Jafari, B. Aricioglu, Nonlinear Dyn. **91**, 957 (2018)
54. Z. Njitacke, L.K. Kengne, Chaos Solitons Fractals **105**, 77 (2017)
55. B. Bao, J. Yu, F. Hu, Z. Liu, Int. J. Bifurc. Chaos **24**, 1450143 (2014)
56. M.P. Hanias, G. Giannaris, A. Spyridakis, A. Rigas, Chaos Solitons Fractals **27**, 569 (2006)
57. A. Wolf, J.B. Swift, H.L. Swinney, J.A. Vastano, Physica D **16**, 285 (1985)
58. K. Diethelm, A.D. Freed, Forschung und wissenschaftliches Rechnen **1999**, 57 (1998)
59. R. Garrappa, *Predictor-corrector PECE method for fractional differential equations.* MATLAB Central File Exchange [File ID: 32918] (2011)
60. M.-F. Danca, Nonlinear Dyn. **81**, 227 (2015)
61. I. Petráš, *Fractional-order nonlinear systems, nonlinear physical science* (Higher Education Press and Springer, Beijing, 2011)
62. M.F. Tolba, A.M. AbdelAty, N.S. Soliman, L.A. Said, A.H. Madian, A.T. Azar, A.G. Radwan, AEU Int. J. Electron. Commun. **78**, 162 (2017)